J O U R N A L O F

Biochemistry
──and──
Molecular Biology

Nucleotide Sequence, Structural Investigation and Homology Modeling Studies of a Ca^{2+}-independent α-amylase with Acidic pH-profile

Reza Hassan Sajedi[1,2], Majid Taghdir[1], Hossein Naderi-Manesh[1,*], Khosro Khajeh[1] and Bijan Ranjbar[1]

[1]Department of Biochemistry and Biophysics, Faculty of Science, Tarbiat Modares University, Tehran, Iran
[2]Department of Biology, Faculty of Science, The University of Guilan, Rasht, Iran

The novel α-amylase purified from locally isolated strain, *Bacillus* sp. KR-8104, (KRA) (Enzyme Microb Technol; 2005; 36: 666-671) is active in a wide range of pH. The enzyme maximum activity is at pH 4.0 and it retains 90% of activity at pH 3.5. The irreversible thermoinactivation patterns of KRA and the enzyme activity are not changed in the presence and absence of Ca^{2+} and EDTA. Therefore, KRA acts as a Ca^{2+}-independent enzyme. Based on circular dichroism (CD) data from thermal unfolding of the enzyme recorded at 222 nm, addition of Ca^{2+} and EDTA similar to its irreversible thermoinactivation, does not influence the thermal denaturation of the enzyme and its T_m. The amino acid sequence of KRA was obtained from the nucleotide sequencing of PCR products of encoding gene. The deduced amino acid sequence of the enzyme revealed a very high sequence homology to *Bacillus amyloliquefaciens* (BAA) (85% identity, 90% similarity) and *Bacillus licheniformis* α-amylases (BLA) (81% identity, 88% similarity). To elucidate and understand these characteristics of the α-amylase, a model of 3D structure of KRA was constructed using the crystal structure of the mutant of BLA as the platform and refined with a molecular dynamics (MD) simulation program. Interestingly enough, there is only one amino acid substitution for KRA in comparison with BLA and BAA in the region involved in the calcium-binding sites. On the other hand, there are many amino acid differences between BLA and KRA at the interface of A and B domains and around the metal triad and active site area. These alterations could have a role in stabilizing the native structure of the loop in the active site cleft and maintenance and stabilization of the putative metal triad-binding site. The amino acid differences at the active site cleft and around the catalytic residues might affect their pKa values and consequently shift its pH profile. In addition, the intrinsic fluorescence intensity of the enzyme at 350 nm does not show considerable change at pH 3.5-7.0.

Keywords: Amino acid sequence, Ca^{2+}-independent α-amylase, Calcium-binding site, Catalytic nucleophile, Modeling, pH profile, pKa

Introduction

Genetic engineering is the most popular method to create new enzymes with improved abilities. On the other hand it is very difficult to design, identify, and improve enzyme properties from the activity and stability point of view mainly due to very little available knowledge concerning their molecular basis (Horikoshi, 1995). The increase in sequence information from newly isolated genes of natural occurring organisms and comparing homologous enzymes with similar folding and function but different properties permit us to identify the molecular determinants and amino acid residues involved in desired features.

α-Amylases (α-1,4-glucan-4-glucanohydrolases, EC 3.2.1.1), which catalyze the hydrolysis of amylose, amylopectin, and related carbohydrates with *endo*-acting property on α-1,4-glycosidic linkages, are among of the most important industrial enzymes with widespread applications (Nielsen and Borchert, 2000; Van der Maarel *et al.*, 2002). α-Amylase can be found with different characteristics depending on the organism of origin, including pH and temperature optima, thermostability, specificity, and their metal ion requirements (e.g. Ca^{2+}) (Nielsen and Borchert, 2000; Pandey *et al.*, 2000). The majority of investigation has been performed on thermostability of α-amylases (Suzuki *et al.*, 1989; Tomazic and Klibanov, 1988; Declerck *et al.*, 2002) and there are a few reports on the other features such as pH-activity and stability and calcium requirement (Nielsen and Borchert, 2000; Tanaka

*To whom correspondence should be addressed.
Tel/Fax: +98-21-8800-9730
E-mail: naderman@modares.ac.ir

and Hoshino 2002; Nielsen *et al.*, 2003; Bessler *et al.*, 2003). Consequently, the structural determinants of these features are highly unknown.

It is the common feature of α-amylases that calcium ion is required for their structural integrity, thermal stability, as well as enzymatic activity (Vallee *et al.*, 1959; Nielsen and Borchert, 2000). It has been shown that the removal of calcium upon adding chelators often lead to a reduction in thermostability and enzyme activity with respect to α-amylases (Violet and Meunier 1989; Hagihara *et al.*, 2001). All X-ray structures of α-amylases so far contain a calcium ion with high affinity at a conserved calcium-binding site, which is located at the interface between domains A and B (CaI) (Boel *et al.*, 1990; Machius *et al.*, 1995; Machius *et al.*, 1998). CaI connects domains A to B and, therefore, contributes to stabilization of the active site structure and controls the formation of the extended substrate-binding site (Machius *et al.*, 1998). This common calcium site is strictly conserved among distantly related α-amylases from mammals (Qian *et al.*, 1994), insects (Strobl *et al.*, 1998), plants (Kadziola *et al.*, 1994), fungal (Swift *et al.*, 1991), and mesophilic (Fujimoto *et al.*, 1998), thermophilic (Suvd *et al.*, 2001), and psychrophilic bacteria (Aghajari *et al.*, 1998). α-Amylase from *Bacillus* sp. KSM-K38 (Amyk38) is an exception, because in this enzyme Na^+ instead of Ca^{2+} plays this crucial role (Nonaka *et al.*, 2003). Additional calcium ions have been found in *Bacillus* α-amylases (Machius *et al.*, 1998; Fujimoto *et al.*, 1998; Brzozowski *et al.*, 2000; Suvd *et al.*, 2001). The second calcium ion (CaII) is located close to the conserved calcium ion (CaI), and in presence of a sodium ion, they form a calcium-sodium-calcium metal triad at the interface of domains A and B. This triadic array exists in *Bacillus licheniformis* α-amylase (BLA) (Machius *et al.*, 1998) and that from closely related *Bacillus* species i.e α-amylase from *B. amyloliquefaciens* (BAA) (Brzozowski *et al.*, 2000) and *B. stearothermophilus* (BStA) (Suvd *et al.*, 2001). A comparison between metal-containing and metal-free form of BLA structures revealed that the loss of metal causes a number of drastic conformational changes around the metal triad and the active site comprising 21 residues. These changes are: In the metal-free form of BLA, the segment between residue 182 and 192, containing Asp183 (a metal-liganding residue), is completely disordered and on the contrary an ordered large loop-like structure forms upon metal binding. Residues 178-182 which contribute to the stabilization of the metal-ligand area by the formation of ionic interaction between Lys180 and Asp202, another metal-liganding residue, undergo a large conformational change. Residues 193-199 are unwound around the metal ions in holo BLA instead of a helical conformation in apo BLA (Machius *et al.*, 1998). The third calcium-binding site (CaIII) is located at the interface of the A and C domains of BLA and BStA (Machius *et al.*, 1998; Suvd *et al.*, 2001).

The active site, located in a cleft at the interface of domains A and B in α-amylases, contains three essential catalytic residues, Asp231, Glu261, and Asp328 (BLA numbering). Two of these, Asp231 and Glu261, are believed to participate in the catalytic mechanism of α-amylases as proton acceptor (nucleophile) and proton donor (acid), respectively (McCarter and Withers 1994; Nielsen *et al.*, 2001; Matsuura, 2002). pH dependence of an α-amylase is determined by the ionization states (in other words the pKa) of the catalytic proton donor and nucleophile residues (Nielsen and Borchert, 2000; Nielsen *et al.*, 2001).

We isolated a Ca^{2+}-independent α-amylase from *Bacillus* sp. KR-8104 (KRA) that is active and stable at low pH and has high resistance toward addition of EDTA (Sajedi *et al.*, 2005). In this study, we investigated sequencing of encoding gene of the α-amylase produced by this strain. The deduced amino acid sequence, thermoinactivation, thermal denaturation, and intrinsic fluorescence measurements of the enzyme were determined and compared to its homologous α-amylases. We also attempted to describe unusual properties of the enzyme using sequence alignment and homology modeling.

Materials and Methods

Materials. α-Amylase from *B. amyloliquefaciens*, 3,5-dinitrosalicylic acid (DNS), PMSF, SDS, EDTA, and Tris were purchased from Sigma (St. Louis). DEAE-Sepharose and phenyl-Sepharose provided by Pharmacia (Uppsala). PCR reagents were obtained from Boehringer Mannheim (Mannheim). Agarose was obtained from GibcoBRL (Maryland) and all other chemicals were from Merck (Darmstadt) and were reagent grade.

Bacterial strain and culture conditions for enzyme production. The bacterial used, *Bacillus* sp. KR-8104, was previously isolated from the soil samples of rhizospher and rhizoplane zone of potato in Karaj, Iran (Sajedi *et al.*, 2005). *Bacillus* sp. KR-8104 was cultured in following medium contaning (gr/L): nutrient broth 8; meat extract 10; soyameal peptone 10; potato starch 10; and NaCl 0.5 for 18 h. The medium used for enzyme production was composed of (gr/L): potato starch 10; soyameal peptone 4; meat extract 3; $CaCl_2 \cdot H_2O$ 0.5; $MgSO_4 \cdot 7H_2O$ 0.3; and K_2HPO_4 1. The time of enzyme production was 60 h and culture was grown at 37°C, in an orbital incubator, with stirring at 180 rpm.

Purification of the enzyme, determination of enzyme activity and protein concentration. KRA was purified from the crude culture supernatants by ammonium sulfate precipitation, ion exchange chromatography on DEAE-Sepharose followed by hydrophobic interaction chromatography on phenyl-Sepharose and concentrating by ultrafiltration as described before (Sajedi *et al.*, 2005). α-Amylase activity was determined at room temperature in 20 mM Tris-HCl, pH 7.4. The concentration of reducing sugars obtained from the catalyzed reaction for 3 min was measured by the dinitrosalicylic acid method according to Bernfeld (Bernfeld, 1955). One unit of α-amylase is defined as the amount of the enzyme that liberates 1.0 μmol of reducing sugar/min with maltose as a standard. Protein concentration was determined by the Bradford method (Bradford, 1976).

Thermal stability studies. The irreversible thermoinactivation of enzyme and influence of Ca²⁺ and EDTA on thermal stability were examined by incubating the enzyme at 70°C in the same buffer in the presence and/or absence of 10 mM CaCl₂ and 5 mM EDTA, for a series of time intervals and cooled on ice. Finally, the residual activity was determined under standard assay conditions.

Circular dichroism measurements for thermal denaturation. The thermal denaturation of enzyme was determined on a JASCO J-715 circular dichroism (CD) spectropolarimeter (Tokyo, Japan) using a 0.2-mg/ml solution of protein. The CD signal at 222 nm as a function of temperature was recorded with a rate of 1°C/min. Results were expressed as molar ellipticity $[\theta]$ (deg cm² dmol⁻¹), based on a mean amino acid residue weight (MRW) assuming average weights of BAA and KRA. The molar ellipticity was determined as $[\theta] = (\theta \times 100 \text{ MRW})/(cl)$, where c is the protein concentration in milligrams per milliliter, l is the light path length in centimeters, and θ is the measured ellipticity in degrees at a wavelength λ. The instrument was calibrated with (+)-10-camphorsulfonic acid, assuming $[\theta]_{291} = 7820$ deg cm² dmol⁻¹ (Schippers and Dekkers, 1981), and with JASCO standard nonhydroscopic ammonium (+)-10-camphorsulfonate, assuming $[\theta]_{290.5} = 7910$ deg cm² dmol⁻¹ (Takakuwa et al., 1985). The data were smoothed using the software, including the fast Fourier transform noise reduction routine that allows enhancement of most noisy spectra without distorting their peak shapes. The melting temperature (T_m) values were determined from the first temperature derivatives of thermal denaturation curves.

Intrinsic fluorescence measurements. Fluorescence measurements were carried out on a Perkin Elmer luminescence spectrometer LS 50B (USA), equipped with a 150 W xenon lamp. Intrinsic fluorescence spectra were recorded between 300 and 400 nm with excitation wavelength of 280 nm at 25°C using a 5-μg/ml solution of protein. The excitation and emission slits both were set at 10 nm.

Primer design, polymerase chain reaction, and sequencing. *Bacillus* sp. KR-8104 total DNA was prepared according to Sambrook et al., (1989) with some modifications. Three overlapping fragments of α-amylase gene were amplified with polymerase chain reaction (PCR) using total DNA as template and the specific primers based on the α-amylase genes of *Bacillus* species from the GenBank. The primers used were 5'-CTGATGCAGTATTTTGAAT GG-3' and 5'-AACTACGATTATTTGATGTATGC-3' for forward primers, 5'-AATTTAATGTGTTTGACAGCATC-3, 5'-ATTGATC ACCTTCCCTCGTC-3', and 5'-TATTACCTTATTTCTGAACATA AATG-3' for reverse primers. PCR experiments were carried out using the conditions recommended by the manufacturer and annealing temperatures were chosen based on the melting temperature of the primers. PCR products for sequencing were recovered from the agarose gels (1% (w/v)) and purified using a DNA extraction kit (MBI Fermentas, Vilnius, Lithuania). Nucleotide sequencing of the α-amylase gene fragments was performed using an automatic sequencer (SEQLAB, Germany) based on dideoxy chain termination method (Sanger et al., 1977). Homology searches were carried out using BLAST N and BLAST P (Altschul et al., 1997) through the NCBI server. Nucleotide and amino acid sequences of α-amylases were derived from the EMBL/

GenBank (Benson et al., 2004) and SwissProt (Bairoch and Apweiler, 1999) databases, respectively. The multiple sequence alignment was performed with the CLUSTAL W program (Thompson et al., 1994). The nucleotide sequence data were submitted to the GenBank under the accession number **AY841124**. Other sequences used in this study were obtained from the GenBank and accession numbers are as follow: *Bacillus licheniformis* (**M38570**) and *Bacillus amyloliquefaciens* (**J01543**) α-amylase gene.

Homology modeling studies and molecular dynamics simulation. The homology study was performed using the MODELLER program ver.7v7 (Marti-Renom et al., 2000). Initially, the KRA sequence was aligned against the BLA sequence with known structure. Due to the good homology, BLA (with protein data bank (PDB) code; **1BLI**) was selected as the template to construct a model of KRA. The resulting KRA structure was relaxed and refined by molecular dynamics simulation with explicit water solvation. MD simulation was performed in the isobaric-isothermal ensemble (NPT) with octahedral periodic boundary condition using the program Amber 8 (Case et al., 2004). The initial model was placed in an octahedral box with about 15000 water molecules. The effective water density in the solvation box was 1.02 g·cm⁻³. 14 Na⁺ charge-balancing-counterions were added to neutralize the existing charges under the protein surface. The simulation began with the 5000 iteration of the energy minimization. Subsequently, MD simulation was performed at 298 K for 1 ns. Analysis and comparison of 3D structures were carried out using Swiss-PdbViewer ver3.7 (Guex and Peitsch, 1997) and MOLMOL (Koradi et al., 1996) programs.

pKa calculations. The MacroDox program (Northrup, 1995) was used to calculate pKa of catalytic residues. All pKa values were calculated in ionic strength 0.1 and temperature 298 K in various pH based on the Tanford-kirwood calculation.

Results and Discussion

KRA was purified using ion exchange and hydrophobic interaction chromatography by DEAE-Sepharose and phenyl-Sepharose column respectively. The fraction corresponding to the active peak related to the chromatogram of phenyl-Sepharose column that combined and concentrated by the ultrafiltration showed homogeneity and appeared as a single band on SDS-PAGE (Fig. 1). The specific activity was improved from 11 U/mg in the concentrated crude culture enzyme to 330 U/mg in purified enzyme (30-fold).

Irreversible thermoinactivation and the effect of Ca²⁺. The time course of inactivation of KRA and BAA at 70°C was determined in 20 mM Tris-HCl, pH 7.4 in the absence or presence of 10 mM Ca²⁺ and 5 mM EDTA. As shown in Fig. 2a, 50 % of its initial activity is retained after 7 min at 70°C. The irreversible thermoinactivation patterns of the enzyme are not changed in the aforementioned conditions. In other words, the thermal stability of the enzyme is not influenced upon
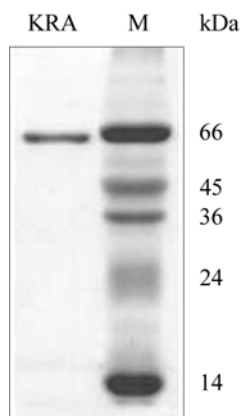
Fig. 1. SDS-PAGE of purified α-amylase from *Bacillus* sp. KR-8104. Lane M, molecular size markers; lane KRA, purified enzyme.

addition of Ca^{2+} and EDTA. However, Ca^{2+} strongly stabilizes BAA, a Ca^{2+}-dependent α-amylase. BAA shows enhanced and reduced thermal stability upon adding 10 mM Ca^{2+} and 5 mM EDTA respectively (Fig. 2b). BAA is completely inactivated after only 3 min of incubation at 70°C in the

presence of 5 mM EDTA. The requirement of calcium ion for thermal stability of BLA and other α-amylases were also reported earlier (Dong *et al.*, 1997; Igarashi *et al.*, 1998). It was also observed earlier that, thermal stability in archaeal α-amylases in the presence and absence of Ca^{2+} were identical (Laderman *et al.*, 1993; Dong *et al.*, 1997).

Thermal denaturation and the effect of Ca^{2+}. To investigate the effect of calcium ion on the thermal denaturation of KRA, CD results from thermal unfolding of the enzyme were recorded in the far-UV region ($\lambda = 222$ nm) with and without added Ca^{2+} and EDTA (Fig. 2c). This experiment was also performed on BAA (Fig. 2d). Thermal unfolding transition for KRA shows a coincidence in the presence of Ca^{2+}, in the presence of EDTA, and in the absence of both of them, as shown in Fig. 2c. Thus, like its irreversible thermoinactivation, adding Ca^{2+} and EDTA does not influence the thermal denaturation of the enzyme and it's T_m. While, the CD experimental data with respect to BAA show significantly different thermal unfolding transition patterns with and without adding Ca^{2+} (Fig. 2d) and EDTA (data not shown). The T_m of BAA is increased approximately 10°C by adding 10 mM Ca^{2+} and decreased approximately 30°C by adding 5
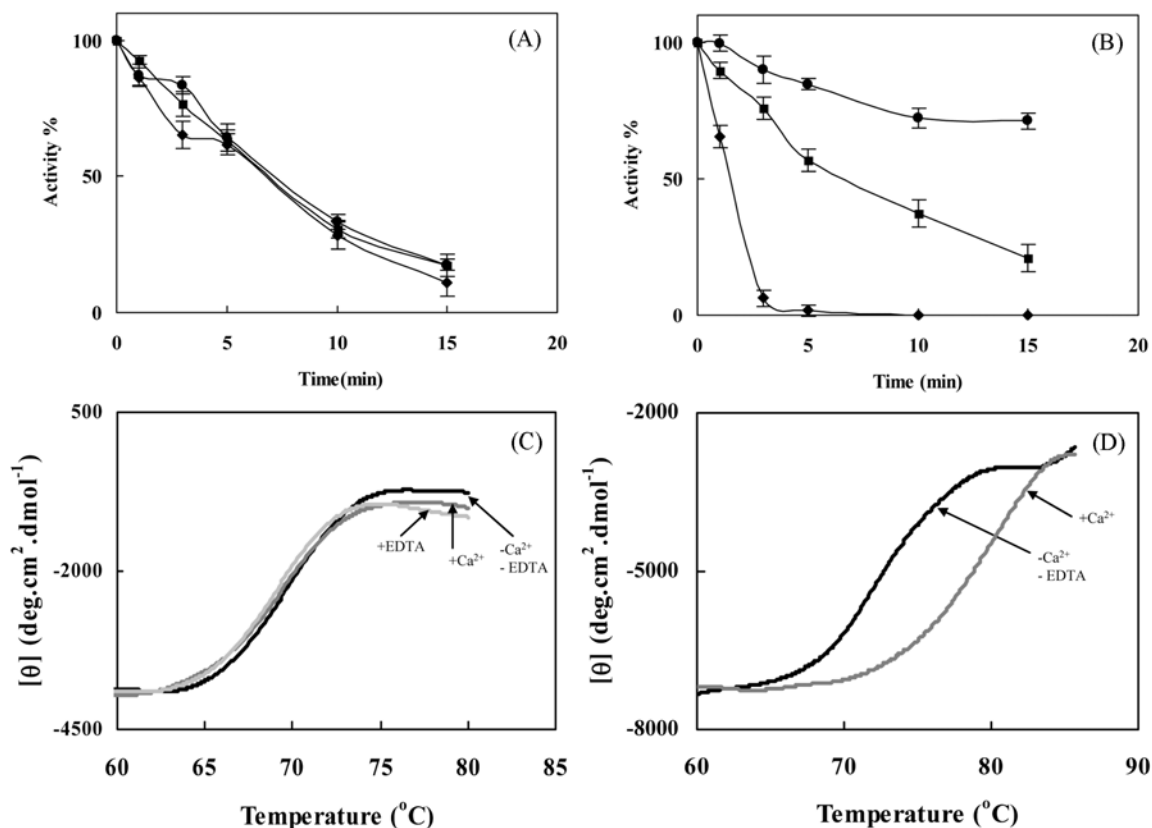

Fig. 2. Irreversible thermoinactivation of KRA (a) and BAA (b) at 70°C in the absence of Ca^{2+} and EDTA (■), in the presence of 10 mM Ca^{2+} (●), and in the presence of 5 mM EDTA (◆) at 70°C and Tris 20 mM, pH 7.4. The experiments were performed in triplicate and bars represent the standard error (S.E.). Thermal unfolding transition as measured by CD technique for KRA (c) and BAA (d) in the absence of Ca^{2+} and EDTA (black), in the presence of 10 mM Ca^{2+} (dark gray), and in the presence of 5 mM EDTA (light gray) in 20 mM Tris buffer, pH 7.4.
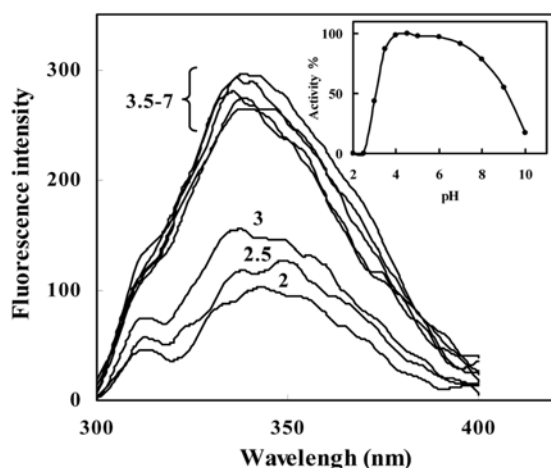
Fig. 3. Fluorescence emission spectra of KRA at different pH values. Spectra were measured at 25°C in 25 mM Glycine-phosphate buffer adjusted in different pH values. The excitation wavelength was 280 nm. The numbers indicate the pH of the samples. The inset is the pH profile of KRA, as indicated in previous paper (Sajedi *et al.*, 2005).

mM EDTA. The tremendous shift of T$_m$ through addition and deletion of Ca^{2+} for BAA, and also BLA was already reported (Khajeh *et al.*, 2001; Fitter and Haber-Pohlmeier, 2004).

Fluorescence intensity and the effect of pH. Our previous report on α-amylase from *Bacillus* sp. KR-8104 shows that KRA is highly active at acidic pH (with its maximum activity at pH 4.0 and 90% of its maximum activity at pH 3.5 (Fig. 3, inset)). Also, it is highly stable at low pH based on determining residual activity (Sajedi *et al.*, 2005). Here, the effect of various pH values on fluorescence intensity has been examined. As BLA and BAA, KRA contains several Trp residues (see Fig. 4). Since the fluorophore Trp is highly sensitive to its surrounding environment, the conformational changes of the enzyme induced with pH changes can be monitored using fluorescence spectroscopy. Figure 3 represents the fluorescence emission spectra of KRA at various pH values with excitation wavelength 280 nm. The results show Trp fluorescence intensity decreases in the pH range from 2.0 to 3.0 (at pH 2, 2.5, and 3.0) as compared to the protein at pH 7.0. While, KRA shows a significant increase in Trp fluorescence intensity at pH 3.5 and 4.0, there are not noticeable changes in the fluorescence intensity above these pH values. These observations indicate the retention of tertiary structure at pH 4.0 and suggest that KRA shows resistance against change of pH in the range from 3.5 to 7.0. On the other hand, BAA shows a significant decrease in Trp fluorescence intensity at pH 4.0 and 5.0, as well as 6.0 when compared to the native protein at pH 7.0, as mentioned in earlier report (Asghari *et al.*, 2004). These results show good parity with our observations based on determination of residual activity at acidic pH and pH-

profile of the enzyme in previous report (Fig. 3, inset) (Sajedi *et al.*, 2005). It may be suggested that pH stability at low pH leads to its performance at this pH.

Nucleotide sequencing of α-amylase encoding gene. To obtain the nucleotide sequence of α-amylase encoding gene, we first designed a set of primers based on the sequences of typical *Bacillus* α-amylase genes such as BLA, BAA, and BSA (*Bacillus subtilis* α-amylase). A 700-bp fragment was amplified by PCR with genomic DNA extracted from *Bacillus* sp. KR-8104 and two of the designed primers and it was then directly sequenced. Nucleotide and deduced amino acid sequence of this fragment showed a high identity with the corresponding part of those from BLA and BAA. To determine the remaining regions of the α-amylase gene sequence, we then designed other primer sets on the basis of the sequence of this fragment and BLA and BAA encoding gene, and two other fragments were amplified and sequenced. The sequence of KRA gene (1328 bp) was determined by overlapping three separate subfragments. Unfortunately, the sequences of 5' and 3' ends of this gene which were equivalent to approximately 20 amino acids at each end of the mature enzyme (when compared to BLA and BAA sequence) was not identified by this method.

Amino acid sequence analysis and comparison. The amino acid sequence of the determined nucleotide sequence was deduced (440 amino acids without 20 amino acids of N- and C-terminus) and compared to that of known α-amylases from *Bacillus* species. In spite of significant differences in thermostability, Ca^{2+}dependency, resistance to EDTA, and pH optima, the deduced amino acid sequence of the α-amylase gene exhibited a very high sequence homology to BAA (85% identity, 90% similarity) and BLA (81% identity, 88% similarity), while interestingly enough a lower degree of homology (58% identity, 73% similarity) was found with a Ca^{2+}-independent and EDTA-resistant α-amylase from *Bacillus* sp. Strain KSM-K38 (AmyK38) (Nonaka *et al.*, 2003). Four highly conserved regions previously identified in α-amylase family (Nakajima *et al.*, 1986; Nielsen and Borchert, 2000) are also existed in this amino acid sequence. The amino acid differences between KR-8104 strain and two reference *Bacillus* α-amylases (BLA and BAA) are dispersed and observed at three different domains. There are some differences in the amino acid sequence of KRA relative to both BLA and BAA. It is important to note that, there is only one amino acid replacement in KRA compared to BLA and BAA in the residues involved in the calcium-binding sites, in spite of a significant difference in its Ca^{2+} dependent behavior. Amino acid numbering and secondary structure nomenclature were done according to those of BLA (Machius *et al.*, 1995; Machius *et al.*, 1998). His406 at the CaIII site of BLA and Pro at putative CaIII site in BAA are replaced by Glu in KRA (Fig. 4). Two residues in BLA, His133 and Ala209, have been previously identified to be important for enzyme thermostability
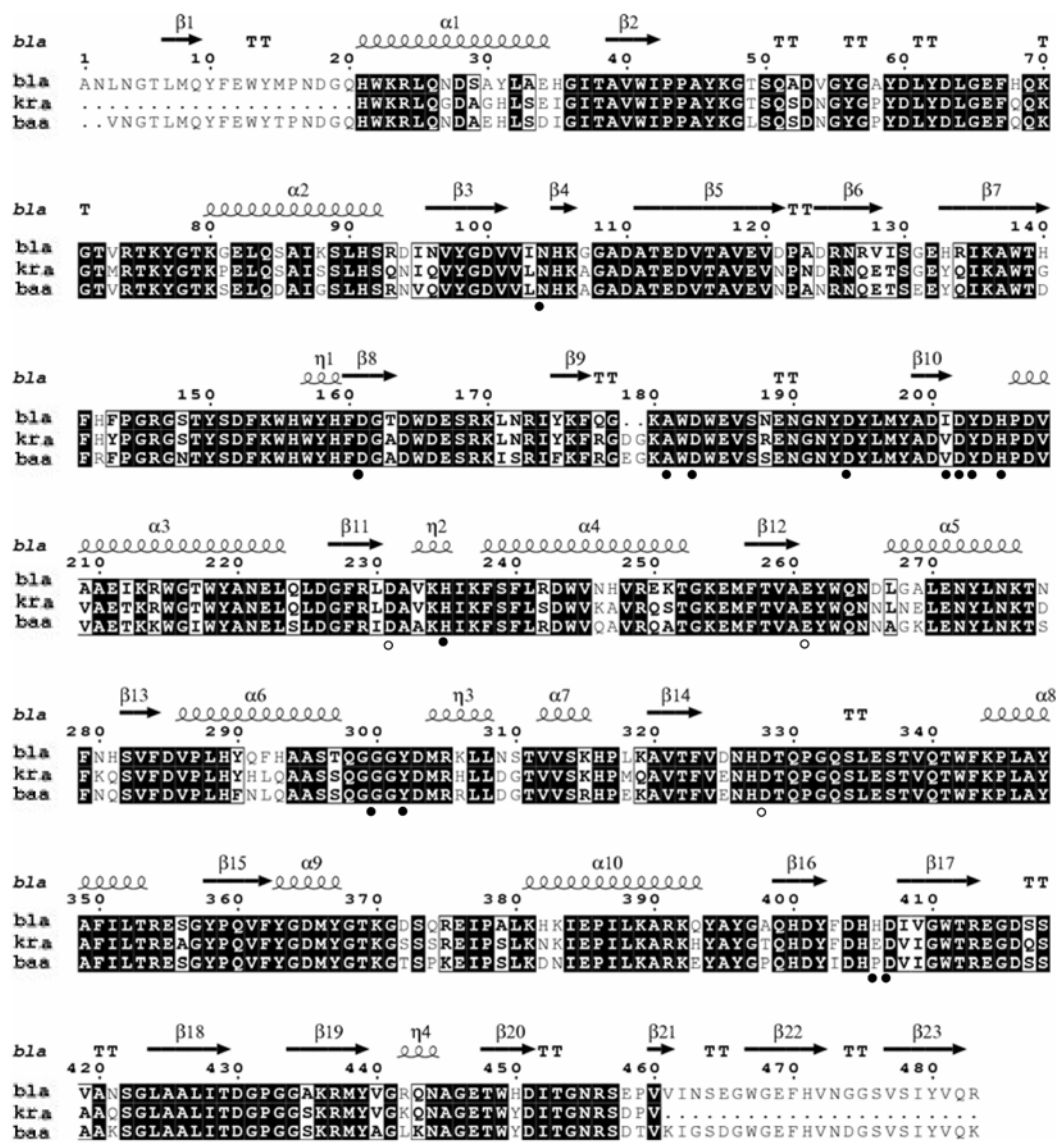
Fig. 4. Amino acid sequence alignment of KRA, BLA, and BAA, presented using the program ESPript (Gouet *et al.*, 1999). The positions of secondary structure elements; α-Helix (α), β-strand (β), 3_{10}-helix (η), and turn (T), catalytic residues (○), and metal-liganding residues (●) (PDB code: **1BLI**) are indicated.

(Declerck *et al.*, 2002). It is very interesting to notice that the His133Tyr and Ala209Val replacements, two of the most stabilizing and cumulative mutations in BLA, occur in KRA at the corresponding positions. In addition, a two-residue insertion seen in BAA and the other homologous α-amylases from *Bacillus* species (Suvd *et al.*, 2001) also found in the amino acid sequence of this enzyme when compared to BLA (Fig. 4). The amino acid substitutions, which lead to alteration of the charge in the enzyme, could be important, such as substitutions in position 93, 188, 242, 246, 269, 278, 280, 291, 320, 382, 396, and 406 of the enzyme.

Prediction of 3D structure of the α-amylase and comparative investigation. To elucidate and understand the Ca^{2+}-independent and acidic pH activity features of the α-amylase, a model of 3D structure of KRA was constructed using the crystal structure of a mutant of BLA, previously determined by Machius et. al. (1998) as a template and MD simulation was performed to refine the initial model. The overall model structure of the α-amylase and substituted residues compared to BLA are presented in Fig. 5. The amino acid differences between two α-amylases are spread out through three domains. The overall structure of KRA is very similar to that of BLA and identically contains three domains, A, B, and C. The $C_α$ Root-mean-square deviation (RMSD) value of the two structures is 0.25Å.

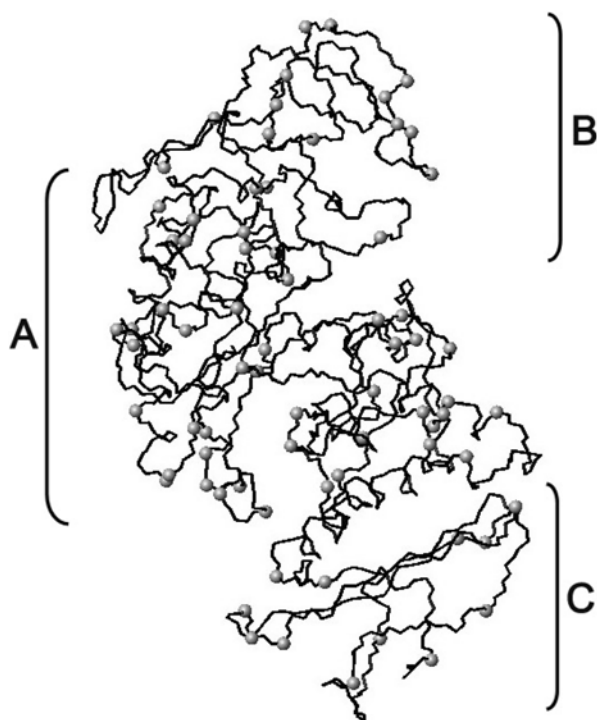**The metal binding sites.** The putative metal-binding sites are

Fig. 5. Overall 3D structure of *Bacillus* sp. KR-8104 α-amylase predicted based on BLA crystal structure (PDB code: **1BLI**), showing the replaced amino acid residues compared to BLA. Domains A, B, and C are indicated by A, B, and C respectively.

Fig. 6. (A) Close up Stereo view of putative metal triad binding site of α-amylase from *Bacillus* sp. KR-8104. The long loop region (residues 178-199) in the substrate- binding cleft (dark green) and two potentially salt bridges at this region are indicated. The distances between C_δ and C atom of guanidinium group of E113-R175 and E269-R188 pairs are calculated as 5.6 and 4.2Å respectively. (B) Superimposition of the amino acid residues involved CaIII binding site in crystal structure of BLA and predicted structure of BAA and KRA.

also found in the constructed model and completely superimposed with those of homologous α-amylase (Fig. 6b for CaIII). However, these sites exhibit large differences in the structure of Ca-free α-amylase from *Bacillus* sp. KSM-K38 (Amyk38) reported earlier (Nonaka *et al.*, 2003). Six Asp residues involved in the metal binding site in BLA are converted to five Asn and one Ser in Amyk38. These replacements will reduce the overall negative charges and induce binding ability to a monovalent metal ion, Na⁺, rather than Ca²⁺. Three Na⁺ ions contribute to the overall enzyme structural integrity. *Pyrococcus woesei* α-amylase (PWA) dose not require the addition of Ca²⁺ for full activity and stability. The molecular basis of its properties is very different. The number of protein ligands in highly conserved calcium-binding site exceeds compare to other α-amylases, which result in high binding affinity to Ca²⁺ for this enzyme. In addition, PWA has a novel Zn-binding site located near to the Ca-binding site essential for enzyme activity and stability (Linden *et al.*, 2003). There are many amino acid differences between BLA and KRA at the interface between A and B domains and around the metal triad and active site (Fig. 5). Most of the charged amino acid substitutions mentioned in the previous section are located at these positions. The two following substitutions at positions 188 and 269 could be interesting and important; Asn188 (in BLA)Ser (in BAA)Arg (in KRA) and Ala269 (in BLA)Asn (in BAA)Glu (in KRA).
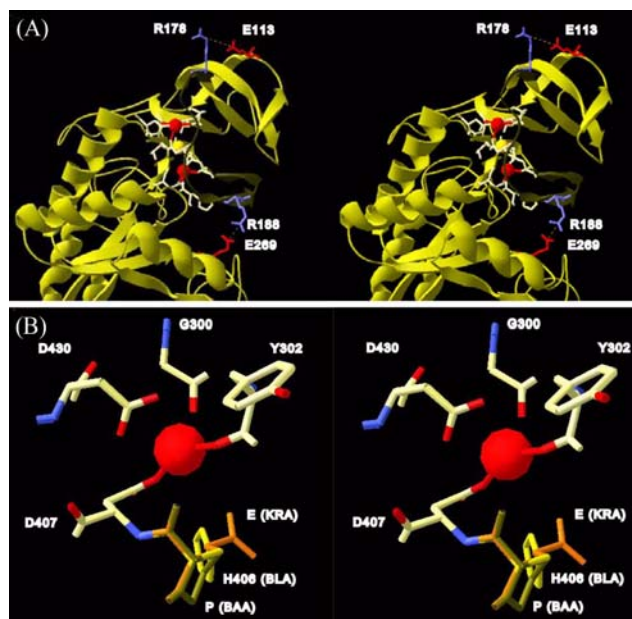
Residue 188 lies in the tip of the long loop region of domain B located in the edge of the substrate-binding cleft between domains A and B while, residue 269 is located in the α-helix α5 in domain A. Machius *et al.* (1998) through comparison between metal-free and metal-containing form of BLA revealed that binding and releasing of metal lead to a large conformational changes in the region comprises 21 residues (178-199) as mentioned in the introduction section. Consequently, it is assumed that stability at this region is essential for the metal binding. In the predicted 3D structure of KRA, Glu269 in the α-helix α5 from domain A located in close proximity to Arg188 from the long loop explained before so that the formation of a salt bridge is possible between them. In addition, the Gly178Arg replacement of this region in KRA structure could provide an additional salt bridge with Glu113 in β-strand β5 of domain B (Fig. 6a). It may be suggested that these alterations could assist the maintaining of the native structure of the loop in the active site cleft and consequently maintenance and stabilization of the putative metal triad binding site. On the other hand, it may be influenced by other replacements around the metal-binding sites and A and B domains interface. The construction of Ca²⁺-insensitive BLA upon amino acid substitutions around the metal triad using site directed mutagenesis in BLA was reported earlier (Hashida and Bisgaard-Frantzen, 2000).
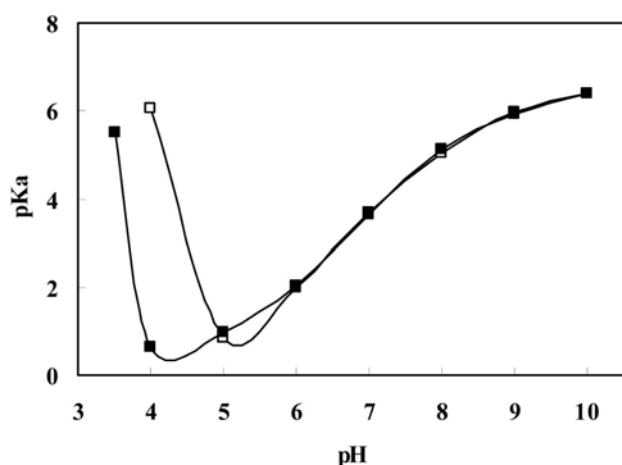
Fig. 7. Calculated pKa values of Asp231 (OD1) for KRA (■) and BLA (□) at different pH.

Table 1. The substituted amino acids that altered charge around Asp231 and the distance between its Cγ and the nearest atom of amino acid side chain (Å)

Residue	Asp231
Lys319Gln	19.6
Arg242Ser	20.6
His293Gln	22.6
His247Ala	20.9
His281Gln	13.2
Asp266Asn	20.3
Asp372Ser	23.0
Asn246Lys	22.8
Ala269Asp	18.3
Asn278Asp	22.9
Asn280Lys	21.8
Asn188Arg	21.4
Gln291His	23.4

Table 2. Neutralneutral amino acid substitutions around Asp231 and the distance between its Cγ and the nearest atom of amino acid side chain (Å)

Residue	Asp231
Ala52Ser	17.6
Val54Asn	10.2
Ile212Thr	13.8
Tyr265Asn	19.1
Gly268Asn	22.6
Thr297Ser	26.8
Ala379Ser	26.4
Ala58Pro	7.4
Gly107Ala	11.8
Thr163Ala	17.7
Ala209val	18.3
Ser320Ala	18.5
Ser356Ala	25.6

There is only one substitution in the residue involved in the third calcium-binding site of KRA at the interface between domains A and C (Fig. 4). His406 in BLA is replaced by Glu in KRA. The corresponding residue in BAA is Pro and the others are conserved (Fig. 6b). This substitution, which is next to Asp407, will provide an electrostatic repulsion between two negatively charged carboxylates that could influence the binding site and, therefore, its overall shape.

The pH-dependence of activity and the pKa calculations. In the following, we have presented a structural interpretation of activity of KRA at low pH. Intrinsic fluorescence results indicate that KRA is stable at low pH (Fig. 3). For activity at extreme pHs, stability alone is not sufficient and the ionization state of the catalytic residues, which depends on the pKa values, must be catalytically suitable too. In α-amylases and closely related enzymes, the proton donor (Glu261) is required to be protonated, while the proton acceptor (Asp231) must be negatively charged (Nielsen and Borchert, 2000; Matsuura, 2002). It is believed that the pH-dependence of α-amylase activity is limited by the protonation of the nucleophile at low pHs and the deprotonation of the proton donor at high pHs (Nielsen *et al.*, 2001). Therefore, the lower the pKa value of Asp231, the higher the α-amylase activity at the low pHs. If the pKa values of the catalytic residues are altered, it is reasonable to assume that the pH-profile will be changed or shifted. There are several microenvironmental determinants of the pKa of a titrable group in proteins such as electrostatic effects, hydrophobic effects (desolvation effects), hydrogen binding, helix dipole interactions, as well as the dynamic aspects of the active site, and altering these factors can influence the pKa. It is already established that the increasing total positive charge or decreasing hydrophobic effects can lead to reduction of the pKa of Asp and Glu (Nielsen *et al.*, 2001; Li *et al.*, 2004).

The catalytic residues in the predicted structure of KRA are

completely superimposed with those of BLA (not shown). Some substituted amino acids around the catalytic residues in KRA lead to the alteration of the charge or hydrophobicity at their side chains as compared to BLA. These substitutions and their distances from catalytic nucleophile (Asp231) are summarized in Tables 1 and 2. The pKa calculations of Asp231 were performed for X-ray structure of BLA and the predicted structure of KRA at different pH values. Fig. 7 indicates the results of these calculations. In KRA, the pKa value of Asp 231 shows a marked decrease at pH 4.0 compared to BLA, whereas, in BLA, such reduction occurs at pH 5.0. These results correspond thoroughly with the pH profiles of KRA (Fig. 3, inset) and BLA (Nielsen and Borchert, 2000). Some replacements around the catalytic nucleophile in KRA are consistent with decreased pKa value as follows: Asn188Arg, Asn246Lys, Asp266Asn, Asn280Lys, and Gln291His (increased positive or decreased negative charges) and Ala52Ser, Val154Asn, Ile212Thr, Tyr265Asn, Thr297Ser, and Ala379Ser (decreased hydrophobic effects). In recent years, although some efforts were carried out to

change the pH-profile and identify its determinants on α-amylases and related enzymes by mutagenesis experiments, the results show very little success and the direction of the pH optima shifts are not correlated with the direction that is reasonable and predictable (Nielsen *et al.*, 1999; Nielsen and Borchert, 2000). These results in combination with the results from fluorescence experiments can describe the observed activity of KRA at acidic pH.

Thus we conclude that although KRA, BLA, and BAA show high identity and similarity in amino acid sequence but there is a great deal of differences in their enzymatic characteristics. The comparison of this enzyme with its homologues enzymes will help us to understand, in more detail, the mechanism that through evolution used to improve or change their properties. This will also help to design better strategy and mutation set up to address the stability, activity, pH-dependence, and Ca requirement of α-amylases. We have tried to shed some light on how and why this enzyme is Ca²⁺-independent and has acidic pH optima by prediction of its 3D structure and comparison with other homologous α-amylases.

References

Aghajari, N., Feller, G., Gerday, C. and Haser, R. (1998) Crystal structures of the psychrophilic α-amylase from *Alteromonas haloplanctis* in its native form and complexed with an inhibitor. *Protein Sci.* **7**, 564-572.

Altschul, S. F., Madden, T. L., Schäffer, A. A., Zhang, J., Zhang, Z., Miller, W. and Lipman, D. J. (1997) Gapped BLAST and PSI-BLAST: a new generation of protein database search programs. *Nucleic Acids Res.* **25**, 3389-3402.

Asghari, S. M., Khajeh, K., Moradian, F., Ranjbar, B. and Naderi-Manesh, H. (2004) Acid-induced conformational changes in *Bacillus amyloliquefaciens* α-amylase: appearance of a molten globule like state. *Enzyme Microb. Technol.* **35**, 51-57.

Bairoch, A. and Apweiler, R. (1999) The Swiss-Prot protein sequence data bank and its supplement TrEMBL in 1999. *Nucleic Acids Res.* **27**, 49-54.

Benson, D. A., Karsch-Mizrachi, I., Lipman, D. J., Ostell, J., Rapp, B. A. and Wheeler, D. L. (2004) GenBank. *Nucleic Acids Res.* **32**, 23-26.

Bernfeld, P. (1955) Amylase, α and β. *Methods Enzymol.* **1**, 149-151.

Bessler, C., Schmitt, J., Maurer, K. H. and Schmid R. D. (2003) Directed evolution of a bacterial alpha-amylase: toward enhanced pH-performance and higher specific activity. *Protein Sci.* **12**, 2141-2149.

Boel, E., Brady, L., Brzozowski, A. M., Derewenda, Z., Dodson, G. G., Jensen, V. J., Petersen, S. B., Swift, H., Thim, L. and Woldike, H. F. (1990) Calcium binding in α-amylases: an X-ray diffraction study at 2.1Å resolution of two enzymes from *Aspergillus. Biochemistry* **29**, 6244-6249.

Bradford, M. M. (1976) A rapid and sensitive for the quantitation of microgram quantitites of protein utilizing the principle of protein-dye binding. *Anal. Biochem.* **72**, 248-254.

Brzozowski, A. M., Lawson, D. M., Turkenburg, J. P., Bisgaard-Frantzen, H., Svendsen, A., Borchert, T. V., Dauter, Z., Wilson, K. S. and Davies, G. J. (2000) Structural analysis of a chimeric bacterial α-amylase, High-resolution analysis of native and ligand complexes. *Biochemistry* **39**, 9099-9107.

Case, D. A., Darden, T. A., Cheatham III, T. E., Simmerling, C. L., Wang, J., Duke, R. E., Luo, R., Merz, K. M., Wang, B., Pearlman, D. A., Crowley, M., Brozell, S., Tsui, V., Gohlke, H., Mongan, J., Hornak, V., Cui, G., Beroza, P., Schafmeister, C., Caldwell, J. W., Ross, W. S. and Kollman, P. A. (2004) AMBER 8, University of California, San Francisco, USA.

Declerck, N., Machius, M., Joyet, P., Wiegand, G., Huber, R. and Gaillardin, C. (2002) Engineering the thermostability of *Bacillus licheniformis* α-amylase. *Biologia, Bratislava.* **57** (Suppl. 11), 203-211.

Dong, G., Vieille, C., Savchenko, A., Zeikus, J. G., (1997) Cloning, sequencing, and expression of the gene encoding extracellular α-amylase from *Pyrococcus furiosus* and biochemical characterization of the recombinant enzyme. *Appl. Environ. Microbiol.* **63**, 3569-3576.

Fitter, J. and Haber-Pohlmeier, S. (2004) Structural stability and unfolding properties of thermostable bacterial α-amylases: a comparative study of homologous enzymes. *Biochemistry* **43**, 9589-9599.

Fujimoto, Z., Takase, K., Doui, N., Momma, M., Matsumoto, T. and Mizuno, H. (1998) Crystal structure of a catalytic-site mutant α-amylase from *Bacillus subtilis* complexed with maltopentaose. *J. Mol. Biol.* **277**, 393-407.

Gouet, P., Courcelle, E., Stuart, D. I. and Metoz, F. (1999) ESPript: analysis of multiple sequence alignments in PostScript. *Bioinformatics* **15**, 305-308.

Guex, N. and Peitsch, M. C. (1997) SWISS-MODEL and the Swiss-PdbViewer: an environment for comparative protein modeling. *Electrophoresis* **18**, 2714-2723.

Hagihara, H., Hayashi, Y., Endo, K., Igarashi, K., Ozawa, T., Kawai, S., Ozaki, K. and Ito, S. (2001) Deduced amino-acid sequence of a calcium-free α-amylase from a strain of *Bacillus. Eur. J. Biochem.* **268**, 3974-3982.

Hashida, M. and Bisgaard-Frantzen, H. (2000) Protein engineering of new industrial amylases. *Trends Glycosci. Glycotechnol.* **68**, 389-401.

Horikoshi, K. (1995) Discovering novel bacteria, with an eye to biotechnological applications. *Curr. Opin. Biotechnol.* **6**, 292-297.

Igarashi, K., Hatada, Y., Hagihara, H., Saeki, K., Takaiwa, M., Uemura, T., Ara, K., Ozaki, K., Kawai, S., Kobayashi, T. and Ito, S. (1998) Enzymatic properties of a novel liquefying α-amylase from an alkaliphilic *Bacillus* isolate and entire nucleotide and amino acid sequences. *Appl. Environ. Microbiol.* **64**, 3282-3289.

Kadziola, A., Abe, J., Svensson, B. and Haser, R. (1994) Crystal and molecular structure of barley α-amylase. *J. Mol. Biol.* **239**, 104-121.

Khajeh, K., Ranjbar, B., Naderi-Manesh, H., Ebrahim Habibi, A. and Nemat-Gorgani, M. (2001) Chemical modification of bacterial α-amylases: changes in tertiary structures and the effect

of additional calcium. *Biochim. Biophys. Acta.* **1548**, 229-237.

Koradi, R., Billeter, M. and Wüthrich, K. (1996) MOLMOL: A program for display and analysis of macromolecular structures. *J. Mol. Graph.* **14**, 51-55.

Laderman, K. A., Davis, B. R., Krutzsch, H. C., Lewis, M. S., Griko, Y. V., Privalov, P. L. and Anfinsen, C. B. (1993) The purification and characterization of an extremely thermostable α-amylase from the hyperthermophilic archaebacterium *Pyrococcus furiosus. J. Biol. Chem.* **268**, 24394-24401.

Li, H., Robertson, A. D. and Jensen, J. H. (2004) The determinants of carboxyl pKa values in turkey ovomucoid third domain. *Proteins* **55**, 689-704.

Linden, A., Mayans, O., Meyer-Klaucke, W., Antranikian, G. and Wilmanns, M. (2003) Differential regulation of a hyperthermophilic α-amylase with a novel (Ca,Zn) two-metal center by zinc. *J. Biol. Chem.* **278**, 9875-9884.

Machius, M., Declerck, N., Huber, R. and Wiegand, G. (1998) Activation of *Bacillus licheniformis* α-amylase through a disorderorder transition of the substrate-binding site mediated by a calcium-sodium-calcium metal triad. *Structure* **6**, 281-292.

Machius, M., Wiegand, G. and Huber, R. (1995) Crystal structure of calcium-depleted *Bacillus licheniformis* α-amylase at 2.2Å resolution. *J. Mol. Biol.* **246**, 545-559.

Marti-Renom, M. A., Stuart, A., Fiser, A., Sánchez, R., Melo, F. and Sali, A. (2000) Comparative protein structure modeling of genes and genomes. *Annu. Rev. Biophys. Biomol. Struct.* **29**, 291-325.

Matsuura, Y. A. (2002) Possible mechanism of catalysis involving three essential residues in the enzymes of alpha-amylase family. *Biologia, Bratislava.* **57** (Suppl. 11), 21-27.

McCarter, J. D. and Withers, S. G. (1994) Mechanisms of enzymatic glycoside hydrolysis. *Curr. Opin. Struct. Biol.* **4**, 885-892.

Nakajima, R., Imanaka, T. and Aiba S. (1986) Comparison of amino acid sequences of eleven different α-amylases *Appl. Microbiol. Biotechnol.* **23**, 355-360.

Nielsen, J. E., Beier, L., Otzen, D., Borchert, T. V., Frantzen, H. B., Andersen, K. V. and Svendsen A. (1999) Electrostatics in the active site of an alpha-amylase. *Eur. J. Biochem.* **264**, 816-824.

Nielsen, J. E. and Borchert, T. V. (2000) Protein engineering of bacterial α-amylases. *Biochim. Biophys. Acta* **1543**, 253-274.

Nielsen, J. E., Borchert, T. V. and Vriend, G. (2001) The determinants of alpha-amylase pH-activity profiles. *Protein Eng.* **14**, 505-512.

Nielsen, A. D., Pusey, M. L., Fuglsang, C. C. and Westh, P. A. (2003) Proposed mechanism for the thermal denaturation of a recombinant *Bacillus halmapalus* α-amylase the effect of calcium ions. *Biochim. Biophys. Acta* **1652**, 52-63.

Nonaka, T., Fujihashi, M., Kita, A., Hagihara, H., Ozaki, K., Ito, S. and Miki, K. (2003) Crystal structure of calcium-free α-amylase from *Bacillus* sp. strain KSM-K38 (AmyK38) and its sodium ion binding sites. *J. Biol. Chem.* **278**, 24818-24824.

Northrup, S. H. (1995) MacroDox v.2.0.2: Software for the Prediction of Macromolecular Interaction. Tennessee Technological University, Cookeville, TN.

Pandey, A., Nigam, P., Soccol, C. R., Soccol, V. T., Singh, D. and Mohan, R. (2000) Advances in microbial amylases. *Biotechnol. Appl. Biochem.* **31**, 135-152.

Qian, M., Haser, R., Buisson, G., Duée, E. and Payan, F. (1994) The

active center of a mammalian α-amylase. Structure of the complex of a pancreatic α-amylase with a carbohydrate inhibitor refined to 2.2 Å resolution. *Biochemistry* **33**, 6284-6294.

Sajedi, R. H., Naderi-Manesh, H., Khajeh, K., Ahmadvand, R., Ranjbar, B., Asoodeh, A. and Moradian, F. (2005) A Ca-independent α-amylase that is active and stable at low pH from the *Bacillus* sp. KR-8104. *Enzyme Microb. Technol.* **36**, 666-671.

Sambrook, J., Fritsch, E. F. and Maniatis, T. (1989) Molecular Cloning: A Laboratory Manual, New York: Cold Spring Harbor Laboratory Press, New York, USA.

Sanger, F., Nicklen, S. and Coulson, A. R. (1977) DNA sequencing with chain-terminating inhibitors. *Proc. Natl. Acad. Sci. USA* **74**, 5463-5467.

Schippers, P. H. and Dekkers H. P. J. M. (1981) Direct determination of absolute circular dichroism data and calibration of commertial instrument. *Anal. Chem.* **53**, 778-788.

Strobl, S., Maskos, K., Betz, M., Wiegand, G., Huber, R., Gomis-Ruth, F. X. and Glockshuber, R. (1998) Crystal structure of yellow meal worm α-amylase at 1.64 Å resolution. *J. Mol. Biol.* **278**, 617-628.

Suvd, D., Fujimoto, Z., Takase, K., Matsumura, M. and Mizuno, H. (2001) Crystal structure of *Bacillus stearothermophilus* α-amylase: possible factors determining the thermostability. *J. Biochem. (Tokyo)* **129**, 461-468.

Suzuki, Y., Ito, N., Yuuki, T., Yamagata, H. and Udaka, S. (1989) Amino acid residues stabilizing a *Bacillus* α-amylase against irreversible thermodenaturation. *J. Biol. Chem.* **264**, 18933-18938.

Swift, H. J., Brady, L., Derewanda, Z. S., Dodson, E. J., Dodson, G. G., Turkenburg, J. P. and Wilkinson, A. J. (1991) Structure and molecular model refinement of *Aspergillus oryzae* (TAKA) α-amylase: an application of the simulated-annealing method. *Acta Crystallogr. D.* **47**, 535-544.

Takakuwa, T., Konno, T. and Meguro, H. (1985) A new standard substance for calibration of circular dichroism: Ammonium d-10-camphorsulfonate. *Anal. Sci.* **1**, 215-225.

Tanaka, A. and Hoshino, E. (2002) Calcium-binding parameter of *Bacillus amyloliquefaciens* α-amylase determined by inactivation kinetics. *Biochem. J.* **364**, 635-639.

Thompson, J. D., Higgins, D. G. and Gibson, T. J. (1994) CLUSTAL W: improving the sensitivity of progressive multiple sequence alignment through sequence weighting, position-specific gap penalties and weight matrix choice. *Nucleic Acids Res.* **22**, 4673-4680.

Tomazic, S. J. and Klibanov, A. M. (1988) Mechanisms of irreversible thermal inactivation of *Bacillus* alpha-amylases. *J. Biol. Chem.* **263**, 3086-3091.

Vallee, B. L., Stein, E. A., Sumerwell, W. N. and Fischer, E. H. (1959) Metal content of α-amylases of various origins. *J. Biol. Chem.* **234**, 2901-2905.

Van der Maarel, M. J., van der Veen, B., Uitdehaag, J. C., Leemhuis, H. and Dijkhuizen, L. (2002) Properties and applications of starch-converting enzymes of the α-amylase family. *J. Biotechnol.* **94**, 137-155.

Violet, M. and Meunier, J. C. (1989) Kinetic studies of the irreversible thermal inactivation of *Bacillus licheniformis* α-amylase. *Biochem. J.* **263**, 665-670.